# DYNAMIC PROCESSES IN A FREE GRANULAR LAYER DURING GAS FILTRATION WITH A SUDDEN PRESSURE DROP

V. A. Antipin, A. A. Borisov, and A. P. Trunev

UDC 532.529.5

Rarefaction waves (RW) in granular fillings have been investigated in [1, 2]. The effects of the pressure in the gaseous phase and of grain size on RW velocity and form were described. The present paper is concerned with propagation of modulated RW in free granular beds of various compositions. The general patterns of behavior of perturbations as a function of the initial parameters of the material were observed. It was discovered that, in a granular filling of any composition, the attenuation coefficient of perturbations increases monotonically with increasing initial pressure. An increase in the grain size at a fixed pressure causes the attenuation coefficient to grow in the range of 7-50 μm and to decrease for grain sizes of 100-1000 μm. A model of these effects has been developed. It is based on expansions of familiar equations for multiphase dynamics [3, 4] near the equilibrium state with respect to a parameter defined as the ratio of gas density to the density of the solid phase. In terms of this model the attenuation coefficient is expressed as a function of problem parameters. The relations are consistent with experimental observations.

1. Experimental Methods and Results. The experiments were conducted in a vertical percussion tube with a diameter of 0.06 m and a length of 1.8 m, which comprised a high-pressure chamber (HPC) and a low-pressure chamber (LPC) 0.9 m long. The general layout of the equipment is illustrated in Fig. 1: 1) LPC, 2) HPC, 3) measurement sensors, 4) triggering sensor, 5) compressed air main valve, 6) pressure gauge, 7) amplifier module, 8) computer, 9) level of granular filling (piston), 10) diaphragm. In the HPC at 0.36, 0.54, and 0.72 m from the lower flange, piezoelectric pressure sensors of an original design (an analog of the LKh601) were mounted which had a passband of $1\text{-}10^5$ Hz (time constant 0.5 sec). The sensors were mounted flush with the working channel wall. Signals from the sensors were sent to the amplifier and then through ADC to an Élektronika-60 microcomputer. According to the experimental conditions, an air gap of 0.15 m was maintained between the top layer of the filling and the membrane. The materials listed in Table 1 were used for filling. The pressure in the LPC was atmospheric; in the HPC it was varied from 0.11 to 0.26 MPa.

The oscillograms of the pressure in cement and aluminum γ-oxide are shown in Figs. 2 and 3 ( $\overline{\Delta p} = p - p_0$, $p_0$ is the initial pressure).

Curves 1-3 (4-6) in Fig. 2 depict the pressure in cement at an initial positive pressure in the LPC of $\overline{\Delta p}$ = 0.04 (0.09) MPa at distances $\Delta x$ = 0.72, 0.54, and 0.36 m from the lower flange, respectively. We will make some comments concerning these curves. After the diaphragm is broken, a pressure pulse with a steep leading edge (shockwave) and a gentle trailing edge is formed in the LPC. Due to the considerable density of the two-phase mixture, the characteristic time of RW penetration into the filling is significantly longer than the time of transmission of the shock pulse through the LPC. As a result of reflection of the shock pulse from the gas/two-phase mixture contact interface, the pressure drop curve is disturbed by an almost harmonic pattern with a period of $T_0 = 2L_1/c_s$, $L_1$ is the LPC length, and $c_s$ is the shock pulse velocity (Fig. 2, curves 1 and 4). As the rarefaction wave front penetrates further into the two-phase mixture, it becomes less steep and, at the same time, the perturbation amplitude decreases (curves 2, 3, 5, and 6).

A similar picture is observed in the propagation of RW into aluminum γ-oxide (d ≈ 50 μm). Curves 1-3 (4-6) in Fig. 3 were recorded at $\overline{\Delta p}$ = 0.03 (0.05) MPa. However, in this case, already at the smallest pressure gradient (~0.01 MPa), perturbations do not penetrate into the filling (in cement, perturbations penetrate throughout the thickness of the layer, even at $\overline{\Delta p}$ = 0.06 MPa). It has been established that the perturbation attenuation

Novosibirsk. Translated from Zhurnal Prikladnoi Mekhaniki i Tekhnicheskoi Fiziki, No. 6, pp. 80-89, November-December, 1990. Original article submitted March 9, 1989; revision submitted June 20, 1989.

 0021-8944/90/3106-0874$12.50 

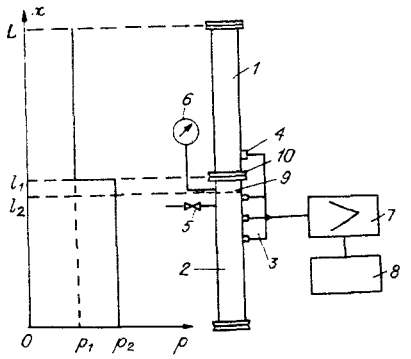


Fig. 1

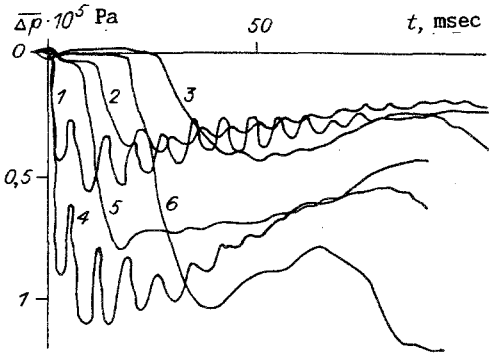


Fig. 2

TABLE 1

| Material | $\rho$, kg/m$^3$ | $\varepsilon$ | d, μm | $d_e$, m/sec | $D_0$, m$^2$/sec |
|---|---|---|---|---|---|
| Aluminum oxide: | | | | | |
| fine | 1188 | 0.7 | 50 | 10.97 | 0.34 |
| coarse-grained* | 732 | 0.65 | 2500 | – | 166 |
| Cement | 985 | 0.56 | 7 | 12.1 | 0.0027 |

*Spherical granules obtained by baking.

coefficient $\varkappa = \ln|A(x_1)/A(x_2)|/|x_1 - x_2|$ (A is the perturbation amplitude) grows monotonically with increasing pressure in the granular fillings of any composition. This is seen, for example, from a comparison of the data in Figs. 2 and 3.

A low propagation velocity is typical for rarefaction waves in finely dispersed granular fillings ($d \lesssim 10^{-4}$ m). As will be shown below, in the case of an equilibrium (in terms of phase velocites), the wave velocity depends on the pressure and density of the mixture according to the expression

$$c_e = \sqrt{p/\varepsilon\rho_c}, \tag{1.1}$$

where $\varepsilon$ is porosity. Thus, under normal conditions in cement $c_e$ = 12.1 m/sec. Expression (1.1) is consistent with the experimental data [2].

Figure 4 represents (1.1). Curves 1 and 2 are the data for cement and aluminum γ-oxide (d = 50 μm), respectively. The values in [1], for a granular filling with a grain diameter of ~14 μm, are slightly higher. We attributed this to the short duration of the pressure pluse (~3 msec), whose velocity may have deviated from an equilibrium level. With the particle size increasing from 7 to 50 μm, $\varkappa$ also grows, but this pattern is suddenly violated at the transition to coarse-grained fillings. In Fig. 3 (curves 7-9) pressure oscillograms describe the propagation of modulated RW in a filling with a grain size of d ~ 2500 μm (aluminum γ-oxide produced by baking); the initial pressure gradient was $\overline{\Delta p}$ = 0.04 MPa. As will be shown below, the rarefaction process in a granular filling in this case is similar to a diffusional process, as can be clearly seen from a comparison of the curves. On the time scale of the process, the delay of signals from sensors immersed in the filling (8 and 9) is negligible compared to signals from the upper sensor (7). Pressure perturbations penetrate the entire thickness of the filling almost simultaneously. Comparing the data in Figs. 2 and 3, we see that $\varkappa$ in aluminum γ-oxide at d ≃ 2500 μm is considerably smaller than at d ≃ 50 μm and comparable to the value of $\varkappa$ in cement.

2. Derivation of Model Equations. In modeling rarefaction waves in a granular filling we proceed from dynamic equations for a two-phase material [3, 4]. In an isothermal approximation,

$$\begin{gathered}\rho_1 d_1\mathbf{u}_1/dt + \varepsilon\nabla p = \varphi_{12}(\mathbf{u}_2 - \mathbf{u}_1) + \rho_1\mathbf{g},\\ \rho_2 d_2\mathbf{u}_2/dt + \rho_2 d_1\mathbf{u}_1/dt + \nabla p = (\rho_1 + \rho_2)\mathbf{g},\\ d_1\rho_1/dt = -\rho_1\mathrm{div}\mathbf{u}_1,\ d_2\rho_2/dt = -\rho_2\mathrm{div}\mathbf{u}_2.\end{gathered} \tag{2.1}$$

Here, $\mathbf{u}_{1,2}$ and $\rho_{1,2}$ are the velocities and densities of the gaseous and solid phases; $d_1/dt = \partial/\partial t + (\mathbf{u}_1\cdot\nabla)$, $d_2/dt = \partial/\partial t + (\mathbf{u}_2\cdot\nabla)$; $\varphi_{12}$ is the parameter of interphase force interaction; g is the vector of mass forces.

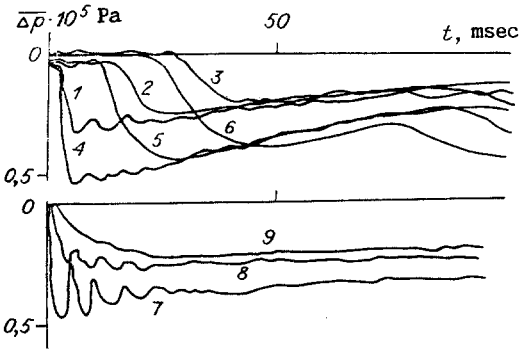


Fig. 3

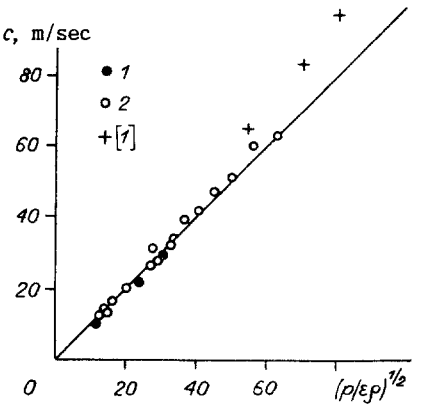


Fig. 4

Equation system (2.1) is closed by relations of flow isothermicity, continuity of the gaseous medium, and incompressibility of particles:

$$p = \rho_g RT,\ T = \text{const};\ \rho_1 = \varepsilon\rho_g;\ \rho_2 = (1-\varepsilon)\rho_s,\ \rho_s = \text{const} \tag{2.2}$$

($\rho_g$ is the true gas density, $\rho_s$ is the density of the grain material, and R is the gas constant).

We will examine the case of a concentrated gas suspension slightly disequilibrated by phase velocities. For this gas suspension the estimates

$$\rho_2 \gg \rho_1,\quad \left|\frac{d_1\mathbf{u}_1}{dt}\right| \sim \left|\frac{d_2\mathbf{u}_2}{dt}\right|. \tag{2.3}$$

take place. These relations may not be satisfied near the gas-filling interface and may not take place for brief processes, as in the experiments of [1]. We further assume that the interface is a thin, light, and rigid piston and the duration of the pressure pulse is sufficiently long. (Some of the above-described experiments were performed expressly to determine the effect of the piston on the process dynamics. However, no significant differences in the behavior of pressure were observed from the results plotted in Figs. 2 and 3.) Applying an estimate of the order of magnitude of (2.3) to the second equation of system (2.1), we find

$$\frac{d_2\mathbf{u}_2}{dt} \approx \left|\frac{\nabla p}{\rho_2}\right|.$$

Hence, and from the first equation of (2.1), follows that, subject to constraint (2.3), the flow of the gaseous medium within terms of the order of $\rho_1/\rho_2 \ll 1$ satisfies the filtration equation

$$\varepsilon\nabla p = \varphi_{12}(\mathbf{u}_2 - \mathbf{u}_1). \tag{2.4}$$

Assume that the interphase interaction coefficient at these flow parameters is not explicitly dependent on phase velocities. Solving (2.4), we write $\mathbf{u}_1 = \mathbf{u}_2 - \varepsilon\nabla p/\varphi_{12}$. With the aid of this result and closing relations (2.2), we rewrite equations for the heterogeneous model of [3]:

$$\begin{aligned} &\rho_2 d\mathbf{u}_2/dt + \nabla p = \rho_2\mathbf{g},\ \partial\rho_2/\partial t + (\mathbf{u}_2\cdot\nabla)\rho_2 = -\rho_2 \operatorname{div}\mathbf{u}_2,\\ &\partial\rho_g/\partial t + (\mathbf{u}_2\cdot\nabla)\rho_g = -(\rho_g/\varepsilon)\operatorname{div}\mathbf{u}_2 + (1/\varepsilon)\operatorname{div}(\varepsilon D_0\nabla p) \end{aligned} \tag{2.5}$$

($D_0 = \varepsilon p/\varphi_{12}$ is the effective diffusivity of the gaseous phase in a heterogeneous medium). By using the hypothesis of flow isothermicity, we can represent the last equation of system (2.5) as

$$\partial p/\partial t + (\mathbf{u}_2\cdot\nabla)p = -(p/\varepsilon)\operatorname{div}\mathbf{u}_2 + (1/\varepsilon)\operatorname{div}(\varepsilon D_0\nabla p). \tag{2.6}$$

Therefore, in an isothermal filling in conditions close to equilibrium the pressure in the material conforms to the law of convective diffusion. The average gas velocity relative to particles is equal to the filtration velocity. We will evalute $D_0$ and determine how it is affected by flow parameters. Previous data on interphase friction in granular beds [4], fillings [5], dust-laden flows [6], and saturated grounds [7], in an approximation linear

TABLE 2

| $f(\varepsilon)$ | Reference | $\varepsilon$ | | | | | |
|---|---|---|---|---|---|---|---|
| | | 0,3 | 0,4 | 0,5 | 0,6 | 0,7 | 0,95 |
| | | $f(\varepsilon)$ | | | | | |
| $633\tau$ | [4] | 443,1 | 380 | 316,5 | 253,2 | 190 | 31,65 |
| $150\tau^2/\varepsilon^2$ | [4] | 816,7 | 337,5 | 150 | 66,7 | 27,6 | 0,42 |
| $180\tau^2/\varepsilon^2$ | [7] | 980 | 405 | 180 | 80 | 33,1 | 0,5 |
| $58,7\tau/\varepsilon^{2,5}$ | [5] | 833,6 | 348 | 166 | 84,2 | 43 | 3,34 |
| $24\tau/\varepsilon^{3,7}$ | [6] | 1445 | 427,5 | 156 | 63,5 | 27 | 1,45 |

with respect to the relative phase velocity, can be represented in the following form:

$$\varphi_{12} = \mu\varepsilon f(\varepsilon)/d^2 \tag{2.7}$$

[$\mu$ is the dynamic gas viscosity, $f(\varepsilon)$ is a certain function]. This linear approximation corresponds to Darcy's law of gas filtration. The diffusivity in (2.5), taking into account (2.7), is expressed by

$$D_0 = pd^2/\mu f(\varepsilon). \tag{2.8}$$

Remarkably, $D_0$ depends on the grain size and is inversely proportional to the gas viscosity. The interphase friction coefficient (2.7) exhibits quite different patterns as a function of porosity or the volumetric gas constant the data of different investigators. The pertinent expressions with specific values and references are given in Table 2, where $\tau$ is the volumetric content of the solid phase ($\tau = 1 - \varepsilon$).

According to Table 2, for air under normal conditions in a granular filling with the root mean square grain size $d \approx 5 \times 10^{-5}$ m, we find $D_0 \approx 14.7\ f(\varepsilon)\ m^2/sec$. At $\varepsilon = 0.5$, according to [4], $D_0 = 0.046\ m^2/sec$; at $\varepsilon = 0.7$, according to [5], $D_0 = 0.34\ m^2/sec$. Without going into the details of these relations, we will note that the data of [4] provide a best approximation of $f(\varepsilon)$ at small $\varepsilon \leq 0.4$; the data of [6] are better at larger values of $\varepsilon$ ($\geq 0.95$). The applicability scope of the remaining results in Table 2 are intermediate between these two extremes.

The postulated isothermicity of the process is affected by experimental conditions. Before the beginning of the experiment, there was no vertical temperature gradient in the granular filling layer. During the process of rarefaction, gas is cooled. However, because of the smallness of the Mach number of the flow ($M_0 \approx c_e/c_s$, $c_s$ is the speed of sound in a pure gas), the change in temperature is so small that it is not registered by a conventional platinum thermocouple. In addition, at comparable specific heat capacities, gas is of an extremely low density compared to the disperse phase, which in this case functions as a thermostat. It can be demonstrated that within terms of the order of $\rho_1/\rho_2$ the temperatures of the gas and the particles in this process are linked by the relation

$$T_1 = T_2 + (\varphi_{12}/\Psi_{12})(u_1 - u_2)^2,$$

where $\Psi_{12}$ is the interphase heat exchange parameter. By using (2.4) and the estimate for the maximum pressure gradient in the form $|\nabla p| \sim p\,\varphi_{12}/c_e$, we can formulate the estimate for the relative change in the gas temperature as

$$\delta T/T \simeq R\varphi_{12}\varepsilon^4 c_e^2/\Psi_{12}c_s^2 \leqslant M_0^2.$$

In cement and in finely dispersed aluminum oxide, $\delta T/T \sim 10^{-3}$, i.e., comparable to the error of model (2.5), which is of the same order of magnitude: $\rho_1/\rho_2 \sim 10^{-3}$.

3. Equilibrium Model. We will consider the limiting form of equations of model (2.5) for $d \to 0$. This case corresponds to fully equilibrated isothermal flow of the mixture. The equations appear as

$$\rho_2 d_2\mathbf{u}_2/dt + \nabla p = \rho_2\mathbf{g},\ d_2\rho_2/dt = -\rho_2 \operatorname{div}\mathbf{u}_2,$$
$$d_2 p/dt = -(p/\varepsilon)\operatorname{div}\mathbf{u}_2. \tag{3.1}$$

As an approximation, we can set $\varepsilon = 1 - \rho_2/\rho_s$. For barotropic motions, setting $p = f(\rho_2)$, we find from the last two equations

$$dp/d\rho_2 = p/(\varepsilon\rho_2), \tag{3.2}$$

Within terms of the order of $\rho_1/\rho_2$ this coincides with the square of the equilibrium sound velocity (see Table 1). For coarse-grained fillings the notion of an equilibrium speed of sound becomes meaningless, as will be explained later.

In the framework of model (3.1), we investigated the following piston problem. In a tube of length L and cross section S, a volume $0 \le x \le \ell_1$ is occupied by a mixture with given values of $\varepsilon$ and $\rho_2$. The volume $\ell_1 < x \le L$ is occupied by a perfect gas with the adiabatic exponent $\gamma$. The cross section $x = \ell_1$ is occupied by a thin piston of mass m. At the initial time the pressure discontinuity is specified in the form of

$$p = \begin{cases} p_2 & \text{at} \quad 0 \leqslant x \leqslant l_2, \quad l_1 < l_2 < L, \\ p_1 & \text{at} \quad l_2 < x \leqslant L, \quad p_1 < p_2. \end{cases}$$

The temperature along the entire length of the tube at t = 0 is constant and equal to $T_0$. We propose to describe the state of the system at T > 0.

The gas dynamic component of the problem was solved by the Lax–Wendroff method in the framework of a perfect gas model. The parameters of the mixture were calculated according to the same scheme with (3.1) applied to a one-dimensional nonstationary flow. The coordinate system is chosen as in Fig. 1, which shows the initial pressure curve. The numeric solutions on the piston were coordinated with its dynamic by means of the equation

$$(p_2 - p_1)S = m\ddot{x}_0 \text{ at } x = x_0(t) \tag{3.3}$$

and were closed by the conditions of gas and mixture nonleakage:

$$\mathbf{u}_1 = \mathbf{u}_2 = \dot{x}_0 \text{ at } x = x_0(t), \ \mathbf{u}_1(L, t) = \mathbf{u}_2(0, t) = 0, \tag{3.4}$$

where S and $x_0$ are the piston area and coordinate; subscript 1 refers to gas. The results of calculations of the decay of gas discontinuity above a cement layer are illustrated in Fig. 5a, where the pressure curves relative to tube length are indicated for the different time points. Initial data: $T_0$ = 300 K; $\varepsilon$ = 0.56; $\rho_2$ = 1250 kg/m$^3$; $p_2$ = 0.1612 MPa; $p_1$ = 0.1 MPa; $\gamma$ = 1.4. We see that the pressure pulse in the gas dynamic section, repeatedly colliding with the piston (curves 1-5), are given for the time points t = 5.6, 10.1, 23.4, 56.1, and 102.6 msec, respectively) produces a modulation of the rarefaction wave: the left-hand side of the curves at $0 \le x \le 1$. The normalized coordinate is

$$\bar{x} = \begin{cases} x/x_0 & \text{at} \quad 0 \leqslant x \leqslant x_0, \\ (x + L - 2x_0)/(L - x_0) & \text{at} \quad x_0 < x \leqslant L. \end{cases}$$

Curves 1-4 in Fig. 5a correspond to the first through fourth reflections of the shock-wave from the piston; curve 5 describes the process stage where the pressure in the gas compartment is practically equalized and the rarefaction wave in the filling has been reflected from the lower flange of the tube. The pressure oscillograms for that time are shown in Fig. 5b, where curves 1-3 correspond to pressures in the cross sections at distances $\Delta x$ = 0.72; 0.54; 0.36 m from the bottom flange. Comparing the curves in Figs. 2 and 5b, we see a fairly good agreement in pressure oscillation period. However, the actual pulse at $\overline{\Delta p}$ = 0.02 MPa attenuates faster than does the calculated pulse at $\overline{\Delta p}$ = 0.0612 MPa. On the other hand, comparing the data in Figs. 3 and 5b, we see that if the modulation wave (MW) is subtracted, the amplitudes of calculated and measured RW correlate with each other. However, at these pressures, the MW does not penetrate at all into an aluminum $\gamma$-oxide filling.

In the framework of an equilibrium model, one can determined the magnitude of the critical pressure gradient at which a supersonic mixture outflow sets in. This value is estimated from a solution of the above piston problem. The piston velocity $\dot{x}_0 = 0$ at t = 0 is constant and equal to $U_0$ at t > 0. As will be seen from the subsequent derivations, the motion of the mixture in this case is self-similar and barotropic. Choosing a coordinate system in such a way that at t = 0 the piston is at rest at the origin, and the axis x' is directed into the interior of the filling, and setting in (3.1) $\xi = x'/t$ is the self-similar variable $\rho_2 = \rho_2(\xi)$, $\mathbf{u}_2 = \mathbf{u}_2(\xi)$, $p = p(\xi)$, we find

$$(\mathbf{u}_2 - \xi)d\rho_2/d\xi + \rho_2 d\mathbf{u}_2/d\xi = 0, \tag{3.5}$$

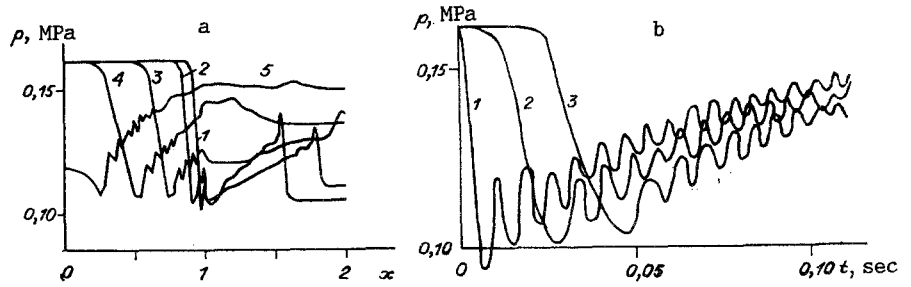

Fig. 5

$$(\mathbf{u}_2 - \xi)\frac{d\mathbf{u}_2}{d\xi} + \frac{1}{\rho_2}\frac{dp}{d\xi} = 0, \quad (\mathbf{u}_2 - \xi)\frac{dp}{d\xi} + \frac{p}{\varepsilon}\frac{d\mathbf{u}_2}{d\xi} = 0.$$

From the first and last equations in (3.5), we derive the expression for the sound velocity squared:

$$dp/d\rho_2 = p/(\varepsilon\rho_2) = c_e^2. \tag{3.6}$$

The solubility condition for system (3.5) is the relationship between mass velocity and sound velocity:

$$\mathbf{u}_2 = \xi \pm c_e. \tag{3.7}$$

In this case, we are concerned with solution of (3.7) $\mathbf{u}_2 = \xi - c_e$. Substituting it into the last equation of (3.5), we find

$$d\mathbf{u}_2/d\rho_2 = c_e/\rho_2. \tag{3.8}$$

Integrating (3.6) and (3.8) and taking into account $\varepsilon = 1 - \rho_2/\rho_s$, we write

$$\begin{gathered} c_e(\rho_2) = c_{e0}\varepsilon_0/\varepsilon, \\ \mathbf{u}_2(\rho_2) = c_{e0}\varepsilon_0 \ln\frac{(1-\varepsilon)\,\varepsilon_0}{(1-\varepsilon_0)\,\varepsilon}, \quad p_2 = p_{20}(1-\varepsilon)\,\varepsilon_0/(1-\varepsilon_0)\,\varepsilon \end{gathered} \tag{3.9}$$

(subscript 0 identifies the parameters of the initial state). Substituting (3.9) into (3.7), we write the law of motion of the mixture in an implicit form:

$$\xi = c_{e0}\varepsilon_0\left(1/\varepsilon + \ln\frac{\varepsilon_0(1-\varepsilon)}{\varepsilon(1-\varepsilon_0)}\right). \tag{3.10}$$

Finally, since we know $\varepsilon = \varepsilon(\xi)$, we can find $c_e(\xi)$, $\mathbf{u}_2(\xi)$. At the point $\xi_0$, where $\mathbf{u}_2(\xi_0) = U_0$, the solution of (3.9) is conjugated with a constant flow as in a similar problem of expansion of a perfect gas under a piston (see, e.g., [8]). From (3.9) we can determine the density or the pressure of the mixture at which for the first time $\mathbf{u}_2 = -c_e$, i.e., a supersonic outflow condition is realized. These parameters are expressed in terms of the solution of the transcendental equation

$$\varepsilon_* \ln\frac{(1-\varepsilon_0)\,\varepsilon_*}{(1-\varepsilon_*)\,\varepsilon} = 1 \tag{3.11}$$

in this form:

$$\rho_2^* = \rho_s(1-\varepsilon_*), \quad p_2^* = p_{20}\varepsilon_0(1-\varepsilon_*)/\varepsilon_*(1-\varepsilon_0)$$

($\varepsilon_*$ is the critical porosity). Hence, at $\varepsilon_0 = 0.7$ and $\varepsilon_* = 0.88$; therefore, $p_2/p_2^* = 3.12$. Note that in a similar problem of polytropic gas flow this ratio is equal to $p_0/p_* = [(\gamma + 1)/2]^{2\gamma/(\gamma-1)}$. Setting $\gamma = 1/\varepsilon_0$ at $\varepsilon_0 = 0.7$, we have $p_0/p_* = 3.65$. Comparing the latter value with the estimate obtained earlier for a granular filling, we see that the flow of the mixture differs little from that of a polytropic gas. This follows from the outward similarity of (3.1) and the model of a gas with a constant ratio of thermal capacities. Importantly, in the above experiments the ratio of pressures required for a supersonic mixture flow should be even greater than the theoretical estimate, because the piston is decelerated at the interaction with the gas in the upper compartment. The data in Figs. 2 and 3 were obtained at $p_2/p_1 \leq 2$. Thus, we know a priori that a supersonic condition of equilibrium flow was not attained in our experiments. This is also confirmed by direct numeric calculations. Nonequilibrium effects must be taken into account to explain these results.

4. Sound Attenuation. In the equations of a nonequilibrium model we set

$$\mathbf{g} = 0,\ \rho_2 = \rho_0 + \tilde{\rho},\ p = p_0 + \tilde{p},\ \mathbf{u}_2 = \mathbf{u}_0 + \tilde{\mathbf{u}}$$

(subscript 0 identifies constant quantities; the tilde identifies the parameters of sound perturbations). Linearizing (2.5) and (2.6) for quantities with the tilde, we obtain in the one-dimensional case

$$\frac{\partial\tilde{\rho}}{\partial t} + \mathbf{u}_0\frac{\partial\tilde{\rho}}{\partial x} + \rho_0\frac{\partial\tilde{\mathbf{u}}}{\partial x} = 0, \tag{4.1}$$

$$\frac{\partial\tilde{\mathbf{u}}}{\partial t} + \mathbf{u}_0\frac{\partial\tilde{\mathbf{u}}}{\partial x} + \frac{1}{\rho_0}\frac{\partial\tilde{p}}{\partial x} = 0,\quad \frac{\partial\tilde{p}}{\partial t} + \mathbf{u}_0\frac{\partial\tilde{p}}{\partial x} + \frac{p_0}{\varepsilon_0}\frac{\partial\tilde{\mathbf{u}}}{\partial x} = D_0\frac{\partial^2\tilde{p}}{\partial x^2}.$$

By virtue of (2.8), here, $D_0 = p_0 d^2/\mu f(\varepsilon_0)$. The values of $D_0$ for different fillings are given in Table 1. For a monochromatic perturbation proportional to $\exp(ikx - i\omega t)$, it follows from (4.1) that

$$(\omega - k\mathbf{u}_0)\left[\frac{p_0}{\rho_0\varepsilon_0}k^2 - (\omega - k\mathbf{u}_0)(\omega - k\mathbf{u}_0 + iD_0k^2)\right] = 0. \tag{4.2}$$

The behavior of $\omega = \omega(k)$, plotted on the basis of (4.2), has three branches. One of them, $\omega = k\mathbf{u}_0$, corresponds to perturbations propagating with the velocity of the main flow; the other two,

$$\omega = k\left(\mathbf{u}_0 \pm c_e\sqrt{1 - D_0^2k^2/c_e^2}\right) - iD_0k^2 \tag{4.3}$$

correspond to sound perturbations. We see from (4.3) that for real wave number values, the frequency is a complex parameter. However, the experimental conditions are such that $\omega$ should be viewed as the real parameter. Instead of (4.3), we will write the initial cubic equation that is not soluble for k [the term in brackets in (4.2)]:

$$i\mathbf{u}_0D_0k^3 + (c_e^2 - \mathbf{u}_0^2 - i\omega D_0)k^2 + 2\mathbf{u}_0\omega k - \omega^2 = 0. \tag{4.4}$$

We set in (4.4) $\mathbf{u}_0 = 0$, which corresponds to sound perturbations in a quiescent medium. Solving it for k, we obtain

$$k = \pm\,\omega e^{i\varphi/2}/(c_e(1 + \mathrm{tg}^2\varphi)^{1/4}), \tag{4.5}$$

where $\varphi = \tan^{-1}(2D_0\omega/c_e^2)$. We assume that the piston vibrates harmonically with a period $T = 2L_1/c_s$ ($L_1$ is the length of the LPC and $c_s$ is the adiabatic sound velocity in the gas). Substituting into (4.5) $\omega = 2\pi/T$, we find the perturbation attenuation coefficient

$$\varkappa = \mathrm{Im}\,k = \frac{\pi c_s}{L_1c_e}\frac{\sin\varphi/2}{(1 + \mathrm{tg}^2\varphi)^{1/4}}. \tag{4.6}$$

It has been established that the function $\varkappa = \varkappa(\varphi)$ has a maximum at $\varphi = \pi/3$. Besides, $\varkappa(0) = \varkappa(\pi/2) = 0$. Therefore, at a certain filling grain size the attenuation of perturbations is maximal. This size can be determined from the condition $2D_0\omega/c_e^2 = \tan\pi/3 = \sqrt{3}$ taking into account (2.8). In particular, for the finely dispersed aluminum $\gamma$-oxide, according to Tables 1 and 2, $\pi D_0c_s/(L_1c_e^2) \approx 3.33$. Here, $\varkappa = 34.5$. By contrast, in cement, where the root mean square grain size $d \approx 7$ μm and $\varepsilon = 0.56$, $D_0 \approx 2.7\cdot10^{-3}$ m$^2$/sec, and $\varkappa \approx 0.84$, which is reasonably consistent with the experimental data. At these parameters the real part of the wave number $\mathrm{Re}\,k = k_0$ is much greater in absolute value than $\varkappa$. We set in (4.4) $k = k_0 + i\varkappa$ and, assuming that the ratio $\varkappa/k_0$ is small ($|\varkappa/k_0| \ll 1$), we represent its solution at $\mathbf{u}_0 \neq 0$ as

$$k = -\frac{\omega(M_e \pm 1)}{c_e(1 - M_e^2)} \mp \frac{iD_0\omega^2}{2c_e^3(1 \pm M_e)^3},$$

where $M_e = \mathbf{u}_0/c_e$ is the equilibrium Mach number. The top sign corresponds to perturbations propagating across the flow; the bottom sign, along the flow. For waves moving from the piston inside the filling,

$$\varkappa = D_0\omega^2/2c_e^3(1 - M_e)^3. \tag{4.7}$$

As can be seen from (4.7), with $M_e$ growing up to unity, $\varkappa$ increases without limit, which explains the behavior of modulated RW in cement (see Fig. 2). Indeed, by virtue of (3.9),

$M_e = \varepsilon \ln(p_2/p_1)$. At $p_2/p_1 = 2$ and $\varepsilon = 0.56$, we find $\varepsilon_* = 0.718$ and $M_e \simeq 0.5$. From (4.7) it follow that $\varkappa$ is increased eightfold over its values at $p_2 \simeq p_1$.

We will examine the behavior of pressure waves in a coarse-grained aluminum oxide. The velocity head of the gas phase at $\overline{\Delta p} \simeq 1$ MPa is insufficient for considerably changing the volume of the filling or for moving it. Therefore, in equations of the nonequilibrium model (2.5) and (2.6), we set $\mathbf{u}_2 = 0$, $\varepsilon = \text{const}$. Now, from (2.6), we obtain an equation familiar from the filtration theory:

$$\partial p/\partial t = \partial(D_0 \partial p/\partial x)/\partial x. \tag{4.8}$$

For monochromatic perturbation of small amplitude, this leads to a simple dispersion equation: $i\omega = D_0 k^2$. Solving it for k, separating the real and imaginary parts, and taking into account the expression for $D_0$, we write the perturbation attenuation coefficient:

$$\varkappa = \sqrt{\omega \mu f(\varepsilon_0)/(2p_0 d^2)}. \tag{4.9}$$

This expression can also be derived directly from (4.6) in the limit $\varphi \to \pi/2$. Calculating $\varkappa$ from Tables 1 and 2, we find $\varkappa \simeq 2.61$. The real part of the wave vector has the same value. Hence, the wavelength of perturbations $\lambda = 2\pi/k_0 \simeq 2.4$ m. These results are consistent with Fig. 3, which shows that a shift in the vibration phase at the distance $\Delta x = 0.18$ m does not exceed 10%; $\varkappa$ varies from 4.7 to 2 for the leading and trailing edges, respectively.

We should note that in real experiments perturbations of finite amplitude were generated. Their interaction with the main flow and each other is more complex than in the foregoing model. A comparison of the curves in Figs. 2 and 3 indicates that, in cement, the perturbations not just attenuate but also contribute to RW amplitude, reducing it substantially. Besides, we know from nonlinear filtration theory [9, 10] that in models of the type of (4.8) perturbations propagate with a finite velocity. This fact, not incorporated into the preceding analysis, is worth further examination.

The authors thank M. E. Gorbunov and O. V. Shapeeva for help with physical and computer experiments.

## LITERATURE CITED

1. B. E. Gel'fand, S. P. Medvedev, A. N. Polenov, et al., "Measurement of the velocity of weak perturbations in porous media of a bulk density," Zh. Prikl. Mekh. Tekh. Fiz., No. 1 (1986).
2. N. A. Azhishchev, V. A. Antipin, A. A. Borisov and V. A. Samoilov, "Rarefaction waves in free granular fillings," Inzh. Fiz. Zh., 52, No. 1 (1986).
3. R. I. Nigmatulin, Dynamics of Multiphase Media [in Russian], Nauka, Moscow (1987).
4. M. A. Gol'dshtik, Transport Processes in a Granular Layer [in Russian], IT Sib. Otd. Akad. Nauk SSSR, Novosibirsk (1984).
5. D. G. Bogoyavlenskii, Fluidics and Heat Exchange in High-Temperature Nuclear Reactors with Spherical Bodies [in Russian], Atomizdat, Moscow (1979).
6. D. J. Carlson and R. F. Hoaglund, "Particle drag and heat transfer in rocket nozzles," AIAA J., 2, No. 11 (1964).
7. V. N. Nikolaevskii, K. S. Basniev, A. G. Gorbunov, and G. P. Zotov, Mechanics of Saturated Porous Materials [in Russian], Nedra, Moscow (1970).
8. L. V. Ovsyannikov, Lectures on the Principles of Gas Dynamics [in Russian], Nauka, Moscow (1981).
9. G. I. Barenblatt, "On certain unstabilized motions of liquids and gas in porous media," Prikl. Mat. Mekh., 16, No. 1 (1952).
10. A. S. Kalashnikov and O. A. Oleinik, "On equations of nonstationary filtration," in: Problems of Filtration Theory and Oil Yield Improvement Mechanics [in Russian], Nauka, Moscow (1987).